ORGANIC PROCESS RESEARCH & DEVELOPMENT
OPR&D
Article
Cite This: Org. Process Res. Dev. XXXX, XXX, XXX−XXX
pubs.acs.org/OPRD

Development of an Efficient Manufacturing Process for E2212 toward Rapid Clinical Introduction

Minetaka Isomura,*[,‡] Taiju Nakamura,[‡] Atsushi Kamada,[†] Takeo Sasaki,[§] Toshiyuki Uemura,[§] Yorihisa Hoshino,[†] Masaaki Matsuda,[†] Yongbo Hu,[∥] Daiju Hasegawa,[§] Kazato Inanaga,[‡] Nobuaki Sato,[§] Kazuhiro Yoshizawa,[‡] George A. Moniz,[∥] Gordon D. Wilkie,[∥] Francis G. Fang,[∥] Yoshihiro Nishikawa,[‡] and Katsuya Tagami*[,‡]

[†]API Research Japan, Pharmaceutical Science & Technology, CFU, Medicine Development Center, Eisai Co. Ltd., 5-1-3-Tokodai, Tsukuba-shi, Ibaraki 300-2635, Japan

[‡]API Research Japan, Pharmaceutical Science & Technology, CFU, Medicine Development Center, Eisai Co. Ltd., 22-Sunayama, Kamisu-shi, Ibaraki 314-0255, Japan

[§]Neurology Tsukuba Research Department, Discovery, Medicine Creation, NBG, Eisai Co. Ltd., 5-1-3-Tokodai, Tsukuba-shi, Ibaraki 300-2635, Japan

[∥]Integrated Chemistry, Eisai AiM Institute, 4 Corporate Drive, Andover, Massachusetts 01810, United States

Supporting Information

ABSTRACT: Process studies of E2212 (**1**) toward rapid clinical introduction are described. Through comprehensive route-finding studies and optimization of key condensation and cyclization steps, a racemate-based manufacturing route was established and successfully scaled-up to the hundred kilogram scale. For the rapid delivery of a drug substance containing the *Z* isomer for preclinical safety studies, the successful scale-up of the photoisomerization of an olefin in a flow system is also presented.

KEYWORDS: *E2212, Alzheimer's disease, γ-secretase, photoisomerization, flow*

INTRODUCTION

Alzheimer's disease (AD) is the most common cause of dementia, constituting a serious social problem that affects the quality of life of the afflicted.[1] It has been hypothesized that senile plaque formed by aggregation of amyloid-*β* protein (A*β*) in patients' brains is a primary cause of AD.[2] In turn, A*β* is produced from amyloid precursor protein (APP) by the function of *β*-secretase and *γ*-secretase. Therefore, intensive R&D studies have been conducted worldwide to develop agents aimed at lowering A*β* by modulation of *β*- and *γ*-secretase.

E2212 (**1**) (Figure 1) is an orally bioavailable *γ*-secretase modulator that was developed as an agent for the treatment of AD.[3] To this end, a reliable and scalable manufacturing process of **1** was required to support drug development activities, including pharmacological and toxicological evaluation as well as formulation development and clinical studies.

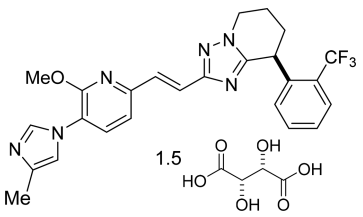

E2212 (1)

Figure 1. Structure of E2212 (**1**).

An initial synthetic route applied by the medicinal chemistry group is shown in Scheme 1.[4] **1** was prepared from its racemic precursor (±)-**5** by chiral chromatography followed by salt formation with D-tartaric acid. Precursor (±)-**5** was obtained from bisamide (±)-**4** via chlorination in $POCl_3$ followed by cyclization in the presence of NH_4OAc. Bisamide (±)-**4** was synthesized by condensation between cyclic hydrazide (±)-**2** and carboxylic acid **3**·TFA.[4]

By means of this route, the initial batches of drug substance for preclinical studies were supplied. However, there were several drawbacks in terms of scalability, especially in the chlorination and cyclization steps: (1) heating (100 °C) in a solvent volume of hazardous $POCl_3$, (2) cyclization at high temperature (140 °C), (3) the use of silica gel chromatography, and (4) resolution by chiral HPLC. Faced with a limited timeline toward initial clinical introduction, process studies of **1** were initiated.

RESULTS AND DISCUSSION

Selection of the Manufacturing Route. To identify the best manufacturing route for future development, comprehensive route-finding studies were attempted. First, a chiral synthetic route was pursued because of its obvious mass throughput advantage over a racemic process requiring chiral

Special Issue: Japanese Society for Process Chemistry

Received: December 15, 2018

DOI: 10.1021/acs.oprd.8b00444
Org. Process Res. Dev. XXXX, XXX, XXX−XXX

Scheme 1. Medicinal Route

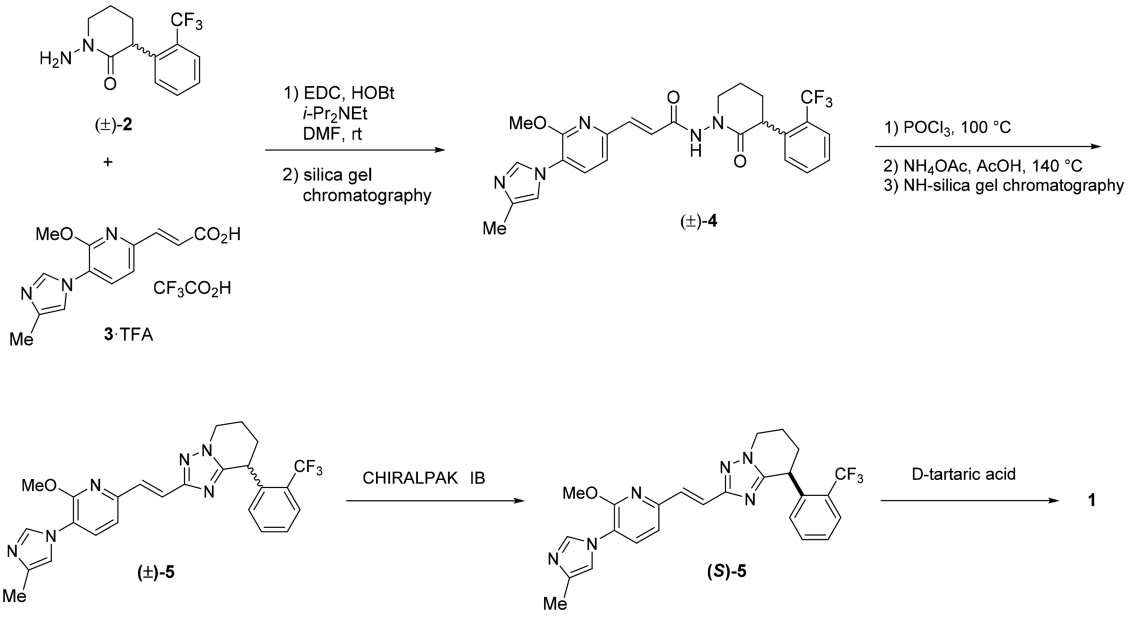

Scheme 2. Summary of Chiral Approaches

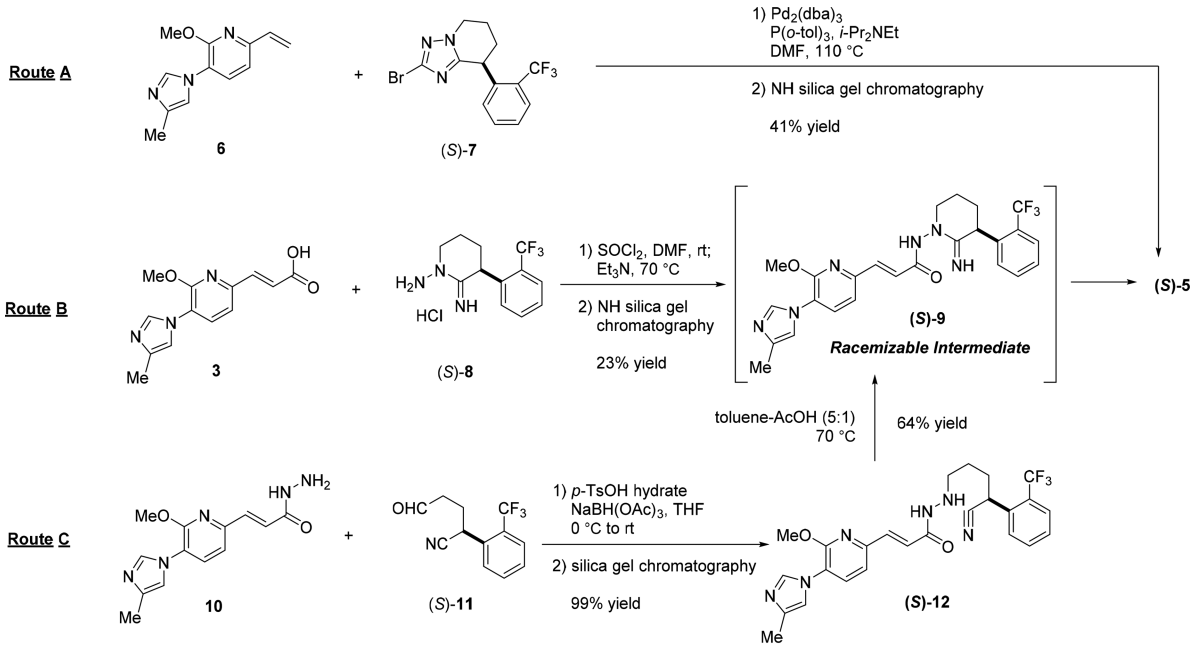

Route	Precursors	Optical Purity (% ee)	
		Precursors	(*S*)-**5**
A	(*S*)-**7**	>97	>95
B	(*S*)-**18**	>99	27
C	(*S*)-**12**	>98	39

resolution. Scheme 2 summarizes three routes (A–C)[5,6] that were deemed feasible through laboratory evaluation.

In each route, coupling precursors (**6**/**3**/**10** as pyridine moieties and (*S*)-**7**/(*S*)-**8**/(*S*)-**11** as chiral moieties) could be prepared from common intermediates, bromide **13**[7] and commercially available carboxylic acid **14**, as shown in Scheme 3. Key coupling reactions between the two moieties proceeded in each route. However, the optical purity of the isolated product (*S*)-**5** was found to be low in Routes B and C even though chiral precursors with high optical purity were used (see the table in Scheme 2). Racemization of the cyclic amidine intermediate (*S*)-**9** was strongly indicated, considering that racemization of (*S*)-**5** did not proceed under these conditions.[8] On the other hand, the Heck coupling between olefin **6** and bromide (*S*)-**7** proceeded without racemization in moderate yield. Thus, of the

DOI: 10.1021/acs.oprd.8b00444
Org. Process Res. Dev. XXXX, XXX, XXX−XXX

Scheme 3. Syntheses of Coupling Precursors

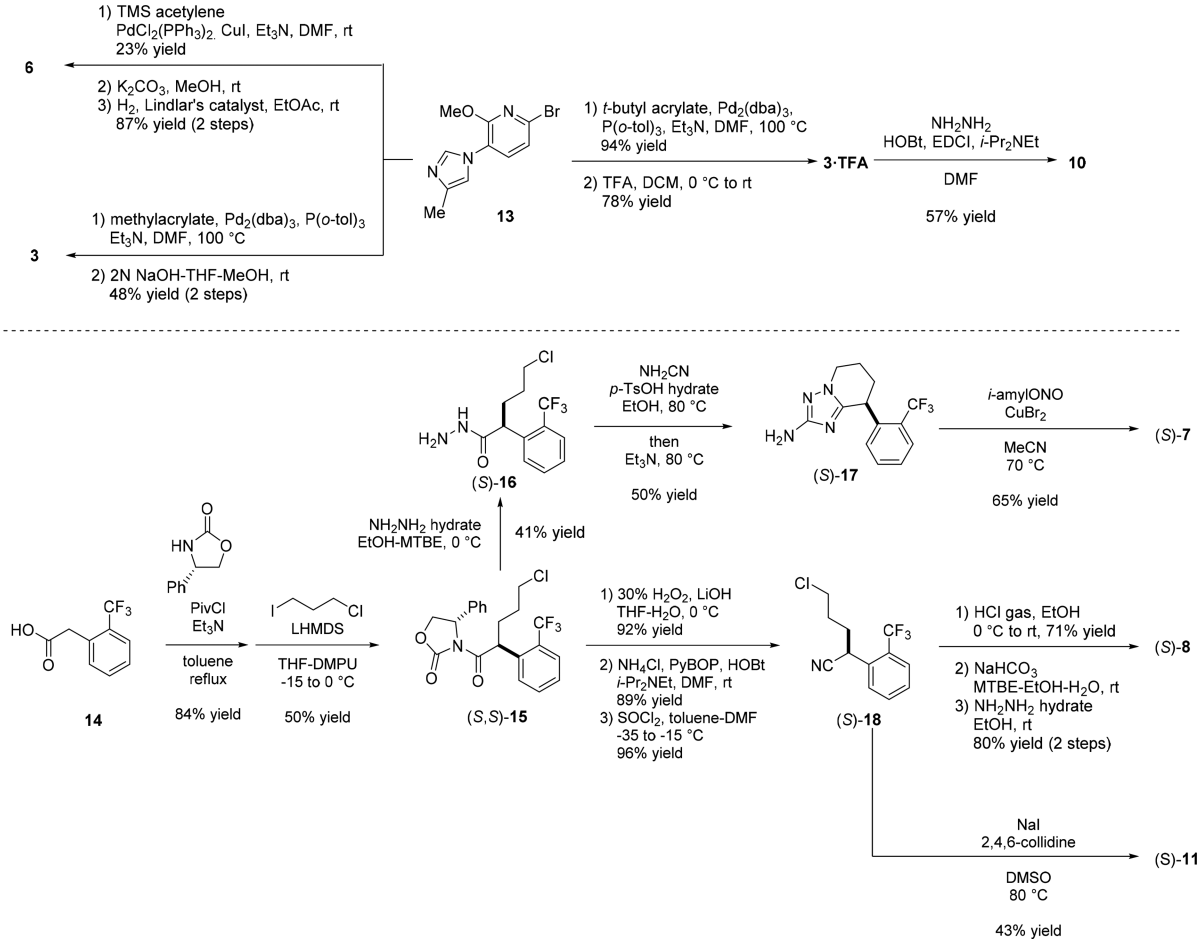

Scheme 4. Chiral Resolution and Recovery Process

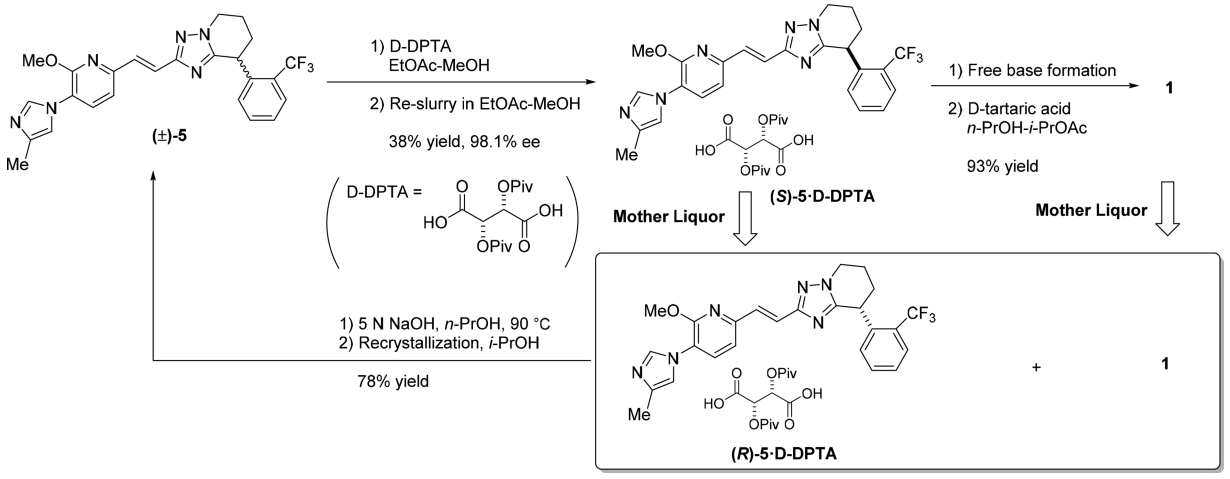

chiral approaches that were attempted, Route A was essentially the only viable candidate.

In parallel with the chiral syntheses, a racemic approach via intermediate (±)-**5** was also explored (Scheme 4). First, diastereomeric salt formation of (±)-**5** was attempted to replace chiral HPLC, which is not suitable for further scale-up. After screening of various chiral acids, dipivaloyl-D-tartaric acid (D-DPTA) was identified as the resolving agent, and the corresponding salt of the desired enantiomer (*S*)-**5**·D-DPTA could be obtained in a practical yield with excellent optical purity.[9] The salt of (*S*)-**5** could be successfully exchanged to D-tartaric acid to give **1** without racemization. Thus, a chiral-salt-based classical resolution process could be established, eliminating the need for HPLC.

Next, recovery of the undesired enantiomer from the mother liquor was attempted. At the outset, it was anticipated that the pK_a of the chiral center would be sufficiently acidic for racemization to occur under basic conditions because of the

DOI: 10.1021/acs.oprd.8b00444
Org. Process Res. Dev. XXXX, XXX, XXX−XXX

Scheme 5. Syntheses of (±)-5

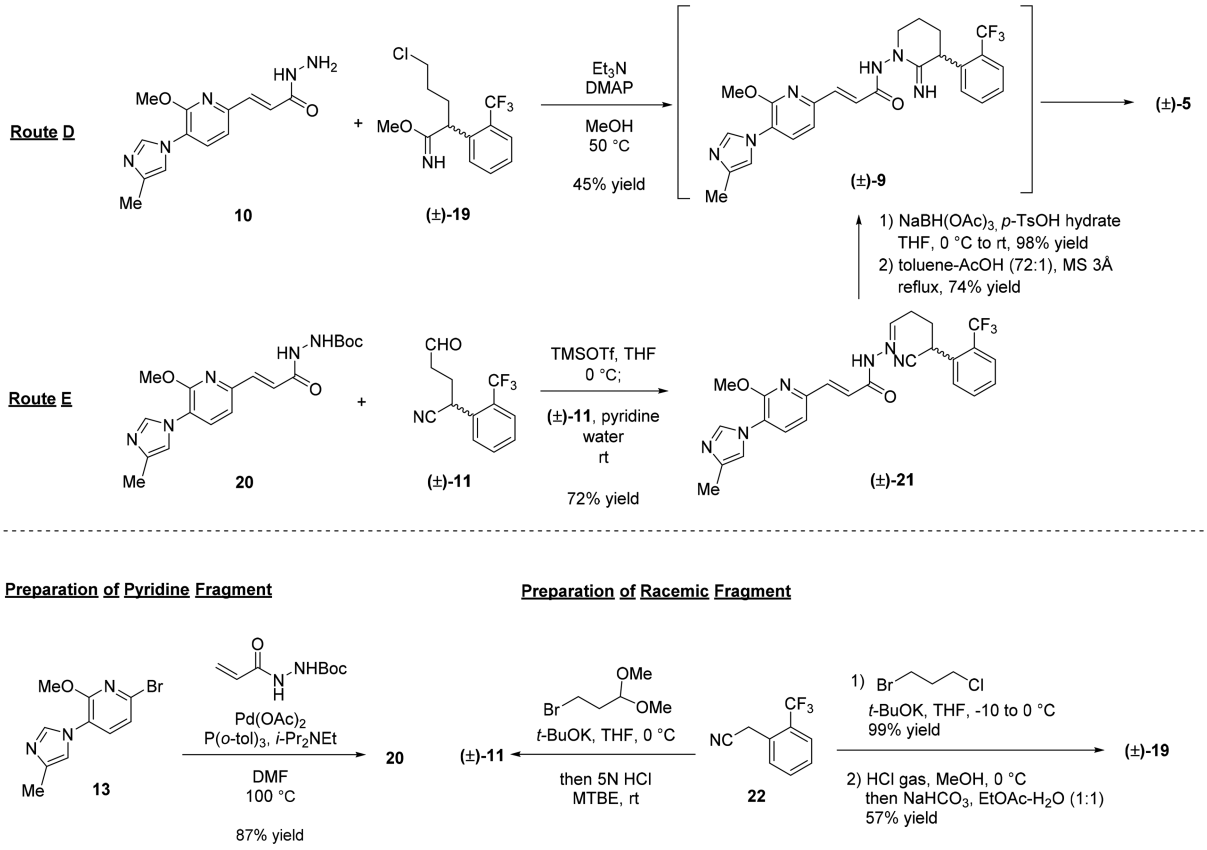

adjacent triazole ring and trifluoromethylphenyl moiety. In the event, racemization of (*R*)-**5** easily proceeded in alkaline solution with heating. During scale-up production, multiple mother liquors containing undesired (*R*)-**5**·D-DPTA and **1** were mixed and racemized by treatment with 5 N NaOH. After extractive workup and recrystallization, (±)-**5** could be recovered in good yield and purity.

Encouraged by the promising performance of the chiral resolution and recovery processes, further synthetic studies to obtain (±)-**5** were continued. Because of the scalability concerns associated with the medicinal chemistry route, Routes D and E were explored (Scheme 5).[6,9]

In both routes, coupling precursors (**10**/**20** as pyridine moieties and (±)-**19**/(±)-**11** as racemic moieties) were easily prepared in one or two steps without silica gel chromatography starting from bromide **13** and commercially available nitrile **22**, respectively (Scheme 5). In both routes, coupling and cyclization via cyclic amidine intermediate (±)-**9** proceeded under mild, scalable conditions to give (±)-**5** in moderate overall yield.

Compared with the chiral approach (Route A), the coupling precursors in the racemic routes can be prepared in fewer steps without silica gel chromatography. In addition, considering that the recovery process of the undesired enantiomer was established (Scheme 4), the overall yield of the racemic approach was expected to be comparable to that of chiral approach. Thus, the racemic approach was selected for further development. In a comparison of Routes D and E, the cost of TMSOTf in Route E was relatively high, and there was also a quality concern associated with the instability of the hydrazone intermediate (±)-**21**. Therefore, Route D was selected as a future development route.

Optimization of the Condensation and Cyclization Phases. After Route D was selected as the manufacturing route for further development, efforts next focused on understanding and optimizing the key cyclocondensation step between hydrazide **10** and imidate (±)-**23**.[10] The reaction consists of two phases: the condensation phase and the cyclization phase (Scheme 6). Major side products that were isolated during optimization studies are also shown in Scheme 6 along with their estimated formation pathways.

Through significant experimentation focused on controlling the reaction pathway to improve the yield, it was recognized that the reaction pathway is highly dependent on the pH of the reaction mixture. Thus, an appropriate choice of base was essential to the success of this reaction, as was stepwise control of the reaction temperature. Selected experimental results showing effects of the base and the temperature are shown in Table 1.

Oxadiazole (±)-**29** is an impurity derived from the condensation phase. This impurity is formed via intermediate (±)-**26**, which in turn is generated from (±)-**24**, the tetrahedral adduct between hydrazide **10** and imidate (±)-**23**. The formation of (±)-**29** and its precursor (±)-**26** increased significantly when no base or less basic pyridine was employed (entries 1 and 4, Table 1), whereas it was almost completely suppressed when a more basic amine (imidazole or Et_3N) was employed (entries 2, 3, 5, and 6). This is presumed to be due to elimination of the amino group of (±)-**24** promoted by protonation in the relatively acidic medium. In addition, the conversion rate of the condensation phase was also strongly

DOI: 10.1021/acs.oprd.8b00444
Org. Process Res. Dev. XXXX, XXX, XXX−XXX

Scheme 6. Reaction Pathway and Major Impurities

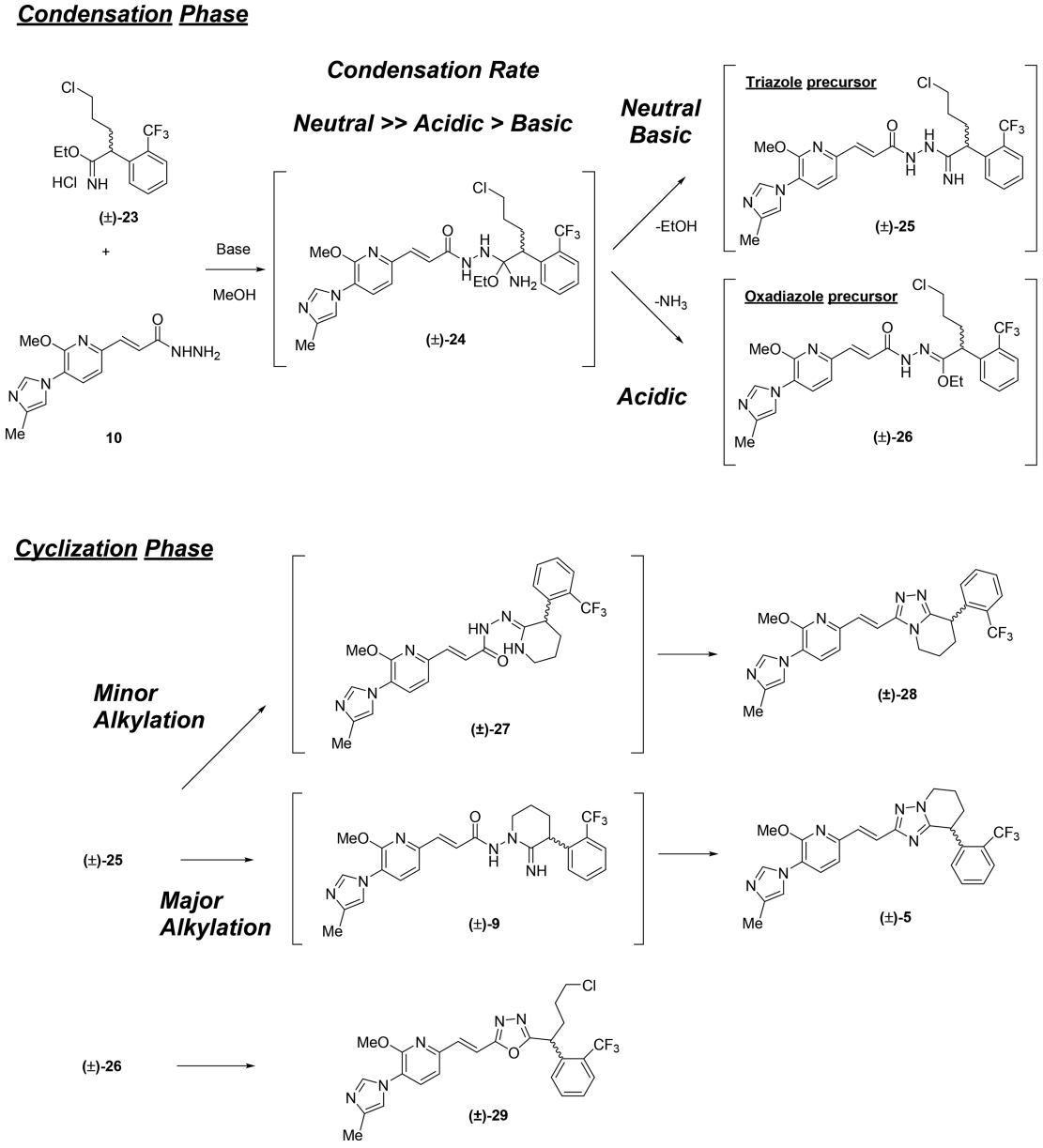

Table 1. Effects of Base and Temperature on the Reaction Profiles

entry	base (equiv)	temp. (°C)	time (h)	hydrazide **10**[a]	triazole condensation (±)-**25**[a]	oxadiazole condensation (±)-**26**[a]	oxadiazole (±)-**29**[a]	desired precursor (±)-**9**[a]	desired (±)-**5**[a]	regioisomer (±)-**28**[a]
1	pyridine (6)	rt	27	17	67	8	3	5	1	0
2	imidazole (6)	rt	27	3	61	0	0	24	12	0
3	Et_3N (6)	rt	27	91	6	0	0	2	1	0
4	none	60	37	20	13	8	42	12	2	2
5	imidazole (3)	60	37	45	9	0	2	0	29	16
6	Et_3N (3)	60	36	82	2	0	1	0	11	4

[a]Each ratio was determined by HPLC area % at 254 nm.

influenced by the amine base added. As shown in Table 1, the condensation was quite slow when 3−6 equiv of Et_3N was used both at room temperature and 60 °C (entries 3 and 6), whereas it proceeded most efficiently when the mixture was buffered with the same amount of imidazole (entry 2).

Another major impurity observed in this reaction is regioisomer (±)-**28**. This impurity is derived from the cyclization phase through competing minor alkylation of (±)-**25**, presumably due to the difference in the inherent reactivities of the two nitrogen atoms in (±)-**25**. The cyclization phase is a slow reaction, thus requiring higher temperature to

DOI: 10.1021/acs.oprd.8b00444
Org. Process Res. Dev. XXXX, XXX, XXX−XXX

Table 2. Selected Results of Optimization Studies

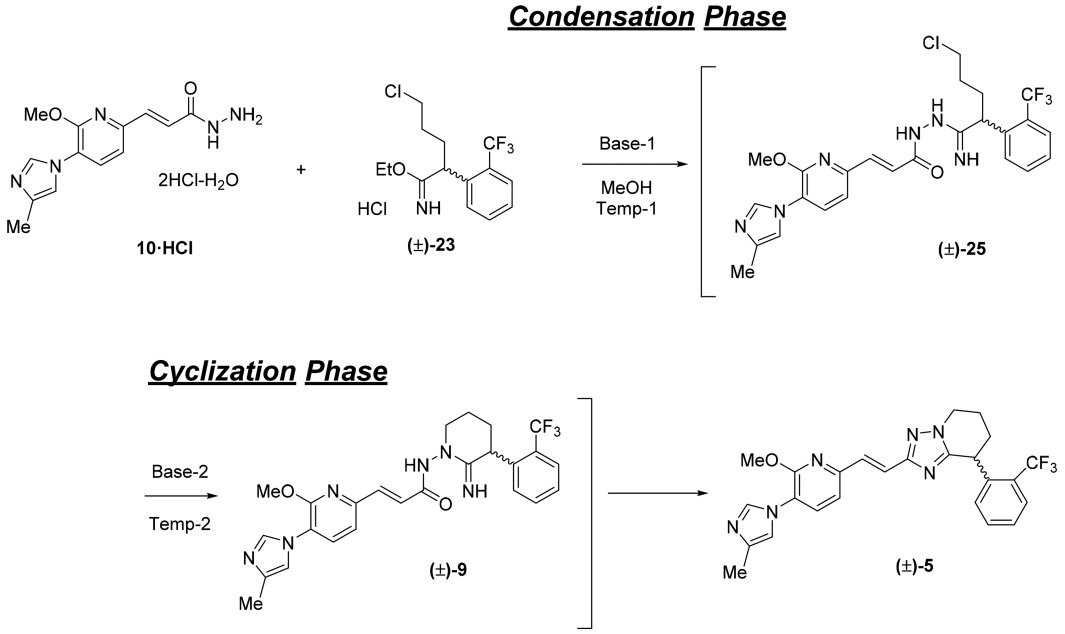

entry[a]	equiv of (±)-23	condensation phase: base 1 (equiv)	condensation phase: temp 1 (°C)	cyclization phase: base 2 (equiv)	cyclization phase: temp 2 (°C)	HPLC area %[b] at 254 nm/271 nm
1	1.0	imidazole (6)	30	none	30	73/–
2	1.0	imidazole (12)	30	none	30	85/–
3	1.0	imidazole (12)	50	none	35	80/–
4	1.0	imidazole (12)	0	none	35	86/90
5	1.2	NaOAc (12)	rt	Et_3N (4)	35	–/94
6	1.2	NaOAc (6)	rt	Et_3N (4)	35	–/94

[a]Each reaction was carried out on a 0.2–1.3 mmol scale. [b]HPLC area % at the end of the reaction. The detection wavelength was changed from 254 to 271 nm through the development studies.

Table 3. Results of Pilot-Plant Production

generation	mass of **10**·HCl (kg)	equiv of imidate (±)-**23**	base 1 (equiv)	temp 1 (°C)	base 2 (equiv)	temp 2 (°C)	HPLC area %[a]	isolated yield (%)
first	21	1.0	imidazole (12)	5–13	none	45	90	58
second	132	1.2	NaOAc (7)	10–15	Et_3N (4)	40–45	96	78

[a]HPLC area % (271 nm) at the end of the reaction.

complete compared with the condensation phase. The regioisomer significantly increased at higher temperature regardless of the basicity of the amine used (entries 4–6), whereas the formation was negligible at room temperature (entries 1–3).

On the basis of these findings, further optimization was performed to identify the best balance among (1) suppression of the oxadiazole formation, (2) adequate condensation rate, and (3) suppression of the regioisomer. Table 2 shows selected experimental results obtained from this optimization effort.

With an equimolar mixture of **10**·HCl and (±)-**23**,[10] opti-optimization studies were carried out, focusing on the HPLC area % at the end of the reaction since it represented the reaction yield well. As shown in entries 1 and 2 in Table 2, increasing the amount of imidazole was effective in keeping the mixture neutral enough to prevent the formation of side products as well as securing good conversion during the condensation phase, increasing the HPLC purity. As shown in entries 2–4, a tendency for decreasing HPLC area % was observed at higher temperature during the condensation phase. To minimize the formation of impurities, the temperature was set as low as operationally possible during the condensation phase. Entry 5 shows that imidazole could be replaced with cheaper NaOAc as a neutralizing base. In addition, slightly increasing the amount of imidate (±)-**23** was effective for complete consumption of hydrazide **10**·HCl. Finally, addition of Et_3N was also effective for accelerating the cyclization phase, thus minimizing the formation of the regioisomer and other unknown impurities to give the highest HPLC purity. This is in contrast to the results in Table 1, entries 3 and 6, where the conversion in the condensation phase was strongly inhibited in the presence of Et_3N. Finally, as shown in entry 6, a comparable result could be obtained by reducing the amount of NaOAc to 6 equiv.

Along with these optimization studies, two scale-up production runs were performed in the pilot plant (Table 3). In the initial pilot batch, the conditions based on entry 4 in Table 2 were employed on a 21 kg scale to afford a reproducible HPLC profile and improved isolated yield (58%) compared with the original conditions (45%; Scheme 5). Subsequently, the optimized conditions based on entry 6 in Table 2 were applied to the second pilot batch on a 132 kg scale to give (±)-**5** in an excellent isolated yield (78%). These scale-up batches

DOI: 10.1021/acs.oprd.8b00444
Org. Process Res. Dev. XXXX, XXX, XXX–XXX

Scheme 7. Isomerization of the Olefin

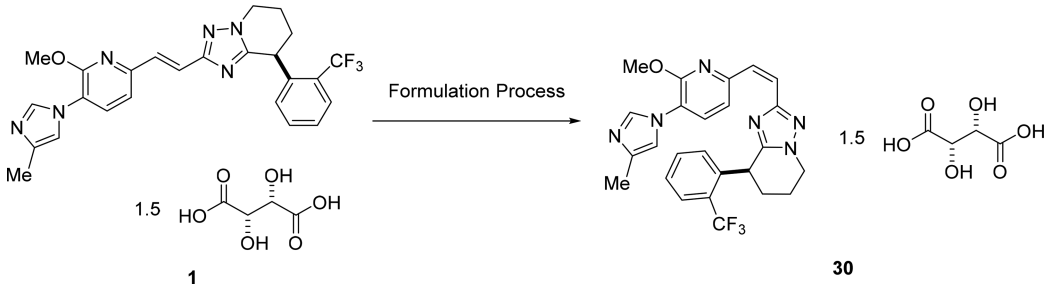

Table 4. Batch Isomerization Experiments

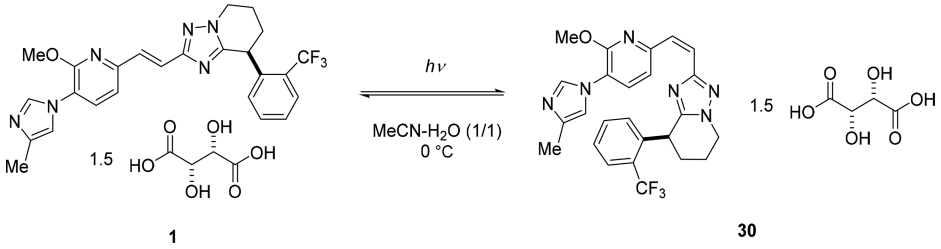

entry	volumes	time	*E*:*Z*:others[a]
1	1000	10 min	54:40:6
2	1000	2 h	38:23:39
3	10	10 min	87:2:11
4	10	2 h	27:7:66

[a]Determined by HPLC area (254 nm).

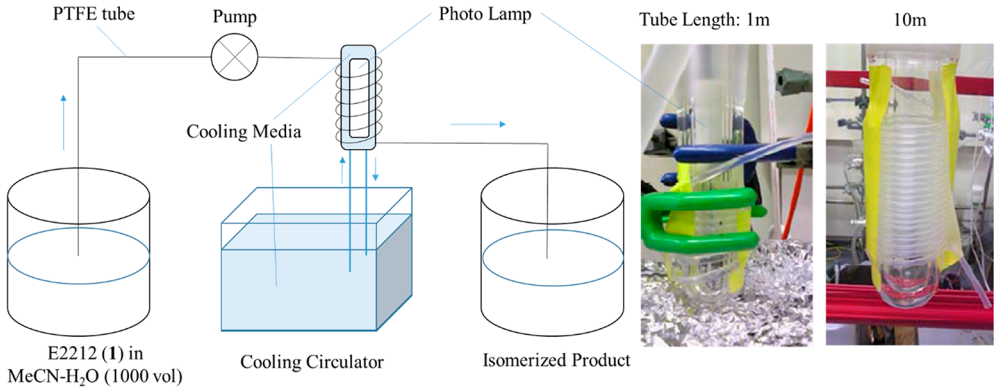

Figure 2. Flow system for photoisomerization.

demonstrated that the process is highly reproducible and robust under mild conditions without requiring special measures in the pilot plant and can easily be applied to manufacturing on a >100 kg scale.

Thus, the rapid establishment of the racemate-based manufacturing process along with the HPLC-free chiral-salt-based resolution, the recovery process, and the optimization of the key condensation and cyclization phases contributed to the timely delivery of a good manufacturing practice (GMP) drug substance that enabled rapid clinical introduction of E2212.

Photoisomerization of the Olefin Using a Flow System. For the fastest introduction into clinical studies, a rapid supply of the drug substance for preclinical safety studies can be as important as establishing a GMP manufacturing process for clinical studies. For E2212 (**1**), it had been confirmed that *E*/*Z* isomerization of the internal olefin proceeded during the formulation process, presumably as a result of exposure to light during operations (Scheme 7). Therefore, supplying the drug substance containing a small amount (target: 1%) of the *Z* isomer **30** to preclinical safety studies was essential to qualify the *Z* isomer before human studies. Faced with a compressed timeline, preparative studies to obtain a sufficient quantity of the *Z* isomer were initiated.

To obtain a sufficient amount of *Z* isomer for preclinical evaluation, a photomediated isomerization of **1** was considered since sufficient material was available. First, preliminary isomerization conditions were explored on a small scale using a commercially available photoreactor (Table 4). These studies revealed that the efficiency of the isomerization was greatly influenced by the solvent volume. Highly diluted (1000 volume) conditions resulted in fast and clean conversion, in contrast to concentrated (10 volume) conditions (entry 1 vs 3). In addition, it was also found that degradation gradually proceeded with extended irradiation time (entry 1 vs 2). To minimize toxicity

DOI: 10.1021/acs.oprd.8b00444
Org. Process Res. Dev. XXXX, XXX, XXX−XXX

risks during the safety studies, it was important that contamination of unknown degradation impurities in the *Z* isomer be minimized. Therefore, a short reaction time under high-dilution conditions was considered necessary.

On the basis of the required quantity of the drug substance for the preclinical safety studies and the target level of the *Z* isomer (1% at 271 nm), isomerization of 185 g of the *E* isomer was required in 185 L (1000 volumes) of solution, which far exceeded the size of the photoreactor available. In addition, on such a large scale it was considered to be impossible to realize a short reaction time since the overall light exposure decreases with increasing volume.

Thus, attention was turned to a flow system. As has been reported in the literature, a photoreaction that is difficult to scale using a traditional batch reactor can be successfully scaled using a flow system.[11] Thus, a single-path flow system consisting of a PTFE tube wound around a traditional photoreactor was installed in the laboratory, as shown in Figure 2. From the inlet of the tube, a solution of **1** in 1000 volumes of MeCN/water was fed using an appropriate pump, and an isomerized *E*/*Z* mixture was eluted from the outlet. Since the lamp generates significant heat during the long irradiation time, a cooling medium was circulated via a circulator to keep the temperature inside the PTFE tube constant throughout the irradiation. By variation of the flow rate and the tube length exposed to light, conversions under various residence times were monitored (Table 5).

Table 5. Photoisomerization Using a Flow System

entry	length (m)	diameter (mm)	flow rate (mL/min)	residence time (s)	*E*:*Z*:others[a]
1	1	2.5	9	33	54:43:3
2	1	2.5	5	60	48:47:5
3	1	2.5	0.5	600	42:45:13
4	10	3.0	184	22	56:39:5

[a]Determined by HPLC area % (254 nm).

With the small-scale flow system using a 1 m length of 2.5 mm diameter PTFE, the isomerization proceeded completely in 10 min (entry 3, Table 5). Since other impurities were detected at higher levels compared with the corresponding batch result (entry 1, Table 4), the residence time was further shortened to assess whether the other impurities could be suppressed while still affording a sufficient *E*/*Z* ratio. As a result, much shorter times (33−60 s) were found to be enough to obtain an acceptable *E*/*Z* ratio with improved HPLC purities (entries 1 and 2). Having identified good conditions for the isomerization with the small-scale flow system, the isomerization was next scaled-up using a longer (10 m) PTFE tube with a wider diameter (3.0 mm) to increase the volume that can be treated within the same working time. As shown in entry 4, comparable results were obtained on the larger scale with almost the same residence time (22 s). Encouraged by the good reproducibility in entry 4, we applied this scale-up setting to the isomerization of ∼185 L of solution of the *E* isomer (185 g) (see the Experimental Section). The feeding and irradiation were completed in 17 h (two working days), and a sufficient quantity of the required *Z* isomer was obtained with the same quality as in the small-scale flow experiment. It should be noted that the continuous cooling of the reaction mixture was important and could be achieved by using a cooling circulator to dissipate the heat generated. Thus, drug substance containing the desired level of the *Z* isomer was successfully delivered for preclinical safety studies on time, which would have been impossible to achieve using traditional batch conditions.

CONCLUSION

Process studies of E2212 (**1**) enabling rapid clinical introduction have been presented. Comprehensive route-finding studies coupled with the chiral-salt-based resolution and enantiomer recovery processes led to the identification of an optimal manufacturing process proceeding via racemate (±)-**5**. Through careful selection of the base and the temperature for a key cyclocondensation process, the various reaction pathways leading to side products were suppressed, and the highly selective formation of the desired racemate (±)-**5** was achieved in excellent isolated yield and quality control. The overall process is mild, operationally simple, and robust and was successfully scaled up to hundred kilogram scale production, contributing to the rapid delivery of GMP drug substance. In addition, the preparation of drug substance containing the *Z* isomer was achieved for the preclinical safety studies. The photomediated isomerization of the internal olefin was also readily scaled up to a multihundred liter scale with excellent reproducibility by applying a rapid (within 1 min) single-path flow irradiation system. A sufficient quantity of the *Z* isomer was rapidly prepared, which would have been difficult to achieve using a traditional batch reaction system.

EXPERIMENTAL SECTION

General. All of the reagents and solvents were obtained from commercial sources, except for the made-to-order bromide **13**. The lamp was a commercially available 450 W high-pressure UV lamp (UM-452, Ushio) fitted with a cooling condenser (Pyrex). The PFA tubing was obtained from commercial sources, and the length and dimensions used for each experiment were as indicated in the text. The experimental procedures and the NMR data for each intermediate in the route-finding studies (Routes A−E) can be found in refs 4, 5, 6, and 9. All of the positive/negative-ion mode electrospray ionization mass spectra were recorded on an LTQ Orbitrap XL mass spectrometer (Thermo Fisher Scientific). With regard to the analytical data for E2212 (**1**), the IR absorption spectrum was measured using an FT/IR-620 spectrometer (JASCO) by the potassium bromide disk method (KBr, IR grade, WAKO, Japan), and the ^{1}H and ^{13}C NMR spectra were recorded on a 600 MHz NMR spectrometer (Bruker AVANCE). For other compounds, the IR absorption spectra were measured using a Spectrum Two FT-IR spectrometer (PerkinElmer), and the NMR spectra were recorded on a 600 MHz NMR spectrometer (Bruker AVANCE III).

Condensation and Cyclization of 10·HCl and (±)-23 (Table 3, First-Generation Process). A reactor was charged with imidate HCl salt (±)-**23** (21.0 kg, 61.0 mol), imidazole (49.6 kg, 728.6 mol), hydrazide dihydrochloride hydrate **10**·HCl (21.1 kg, 60.9 mol), and MeOH (83.2 kg). The mixture was stirred at 5−14 °C for 24 h and then warmed to 45 °C and stirred for an additional 17 h. Upon reaction completion, the mixture was cooled to room temperature. Half of the reaction mixture was drained and kept in another reactor while the remaining half of the mixture was diluted with EtOAc (94.4 kg), 15% aqueous NaCl (63.0 kg), and 5 N HCl (34.1 kg) while the internal temperature was kept below 35 °C. The pH was confirmed to be 6.5−7, and the layers were separated. To the organic phase was added 30% aqueous $NaHSO_3$ (63.1 kg), and the solution was

DOI: 10.1021/acs.oprd.8b00444
Org. Process Res. Dev. XXXX, XXX, XXX−XXX

warmed to 60 °C for 0.5 h. The solution was cooled to 30 °C, and the aqueous layer was separated. To the organic phase was added cooled 5 N HCl (56.9 kg), and after the pH was confirmed to be 0, the organic phase was separated. The aqueous phase was added back into the reactor, and EtOAc (94.6 kg) and MeOH (4.2 kg) were added. The resulting mixture was cooled to 7 °C followed by the addition of cooled 5 N NaOH (75.6 kg) while the internal temperature was maintained below 20 °C. The pH was confirmed to be 6.0−6.5. The aqueous layer was separated, and the organic layer was washed with 5% aqueous $NaHCO_3$ (53.6 kg) and MeOH (4.2 kg). The pH was confirmed to be 8.5. The layers were separated, and the organic layer was washed with 5% aqueous NaCl (32.8 kg) and MeOH (4.2 kg). The aqueous layer was separated and washed with water (31.5 kg). The aqueous layer was separated, and MeOH (4.2 kg) was added to give organic solution 1. The remaining half of the reaction mixture kept in another reactor was processed with the same process as described above to give organic solution 2. Organic solutions 1 and 2 were combined, and the organic layer was filtered through a Zeta Carbon 35SP CUNO filter. The filter was rinsed with EtOAc (57.2 kg). The organic layer was concentrated under reduced pressure at 35−40 °C. The residue was azeotroped with *i*-PrOH (33.0 kg × 3). The residue was redissolved in *i*-PrOH (66.2 kg) at 70−80 °C. A seed crystal (50.4 g) was added at 57 °C. The mixture was cooled to −5 to 0 °C at a rate of 10 °C/h and held at −5 to 0 °C. The crystals were filtered, rinsed with 1:1 *i*-PrOH/*n*-heptane (25.0 kg), and dried under reduced pressure at 60 °C to give crystals of the racemate (±)-**5** (19.0 kg, including 10.4% solvents and water, 58.3% yield from **10**·HCl) as a white powder. FTIR (cm^{-1}, KBr) 3435, 2952, 2867, 1571, 1505, 1454, 1315, 1163, 1112, 973, 814, 773; ^1H NMR (600 MHz, $CDCl_3$) δ 7.99 (d, J = 1.2 Hz, 1H), 7.75 (d, J = 7.6 Hz, 1H), 7.67 (d, J = 15.8 Hz, 1H), 7.51 (dd, J = 7.6, 7.5 Hz, 1H), 7.49 (d, J = 7.8 Hz, 1H), 7.46 (d, J = 15.8 Hz, 1H), 7.42 (dd, J = 7.8, 7.5 Hz, 1H), 7.04 (d, J = 7.8 Hz, 1H), 6.97 (dd, J = 1.2, 0.8 Hz, 1H), 6.96 (d, J = 7.8 Hz, 1H), 4.74 (dd, J = 8.4, 6.0 Hz, 1H), 4.39 (br ddd, J = 13.0, 7.4, 5.5 Hz, 1H), 4.35 (ddd, J = 13.0, 8.9, 5.0 Hz, 1H), 4.06 (s, 3H), 2.45 (dddd, J = 13.2, 6.7, 6.7, 2.5 Hz, 1H), 2.32 (d, J = 0.8, 3H), 2.30 (m, 1H), 2.19 (m, 1H), 1.98 (dddd, J = 13.6, 11.0, 8.3, 2.8 Hz, 1H); ^{13}C NMR (150 MHz, $CDCl_3$) δ 160.7, 155.9, 155.0, 150.6, 140.3, 138.5, 136.7, 132.3, 132.1, 131.1, 130.1, 128.4 (q, J_{C-F} = 29.8 Hz), 127.3, 126.3 (q, J_{C-F} = 5.6 Hz), 124.5 (q, J_{C-F} = 274.0 Hz), 122.4, 120.9, 116.6, 115.9, 53.8, 47.4, 37.8, 31.2, 21.3, 13.7; HRMS (ESI+) calcd for $C_{25}H_{24}F_3N_6O$ ($[M + H]^+$) 481.1958, found 481.1959. HPLC conditions to monitor the reaction: XBridge-Shield-RP18 (5 μm, 4.6 mm × 250 mm), 1.0 mL/min, oven temperature = 40 °C, UV detection at 271 nm, mobile phase A = 900:100:1 v/v/w H_2O/MeCN/$AcONH_4$, mobile phase B = 100:900:1 v/v/w H_2O/MeCN/$AcONH_4$, gradient (time (min)/B conc (%)) = 0/5 → 5/45 → 30/45 → 35/100 → 40/100 → 40.01/5 → 47/stop, relative retention time (RRT) of hydrazide (**10**) = 0.29, RRT of intermediate (±)-**25** = 0.39, RRT of intermediate (±)-**9** = 0.72.

Characterization of Oxadiazole (±)-29. FTIR (cm^{-1}, KBr) 3419, 2952, 1588, 1499, 1403, 1313, 1120, 1036, 964, 821, 770, 736; ^1H NMR (600 MHz, $CDCl_3$) δ 7.82 (d, J = 1.3 Hz, 1H), 7.74 (d, J = 7.9 Hz, 1H), 7.58 (d, J = 15.7 Hz, 1H), 7.58 (m, 1H), 7.58 (m, 1H), 7.53 (d, J = 7.7 Hz, 1H), 7.42 (br dd, J = 7.9, 7.9 Hz, 1H), 7.36 (d, J = 15.7 Hz, 1H), 7.03 (d, J = 7.7 Hz, 1H), 6.98 (dd, J = 1.2, 0.9 Hz, 1H), 4.67 (dd, J = 7.6, 7.6 Hz, 1H), 4.07 (s, 3H), 3.57 (ddd, J = 6.6, 6.3, 2.2 Hz, 2H), 2.54 (dddd, J = 13.6, 10.7, 8.3, 5.1 Hz, 1H), 2.30 (d, J = 0.9 Hz, 3H), 2.29 (m, 1H), 1.99 (m, 1H), 1.77 (m, 1H); ^{13}C NMR (150 MHz, $CDCl_3$) δ 166.9, 164.6, 156.0, 148.3, 138.8, 137.3, 136.6, 136.1, 132.7, 132.0, 129.2, 128.5 (q, J_{C-F} = 29.7 Hz), 127.9, 127.0, 126.3 (q, J_{C-F} = 5.6 Hz), 124.3 (q, J_{C-F} = 273.9 Hz), 122.5, 121.5, 118.1, 115.7, 113.9, 54.1, 44.2, 38.0, 32.3, 30.3, 13.7; HRMS (ESI+) calcd for $C_{25}H_{24}ClF_3N_5O_2$ ($[M + H]^+$) 518.1565, found 518.1573.

Characterization of Regioisomer (±)-28. FTIR (cm^{-1}, KBr) 3412, 2955, 1581, 1499, 1450, 1403, 1310, 1158, 1118, 1034, 961, 784; ^1H NMR (600 MHz, $CDCl_3$) δ 7.82 (d, J = 1.3 Hz, 1H), 7.72 (d, J = 7.8 Hz, 1H), 7.68 (d, J = 15.6 Hz, 1H), 7.54 (d, J = 7.6 Hz, 1H), 7.53 (d, J = 15.6 Hz, 1H), 7.47 (dd, J = 7.8, 7.6 Hz, 1H), 7.38 (dd, J = 7.8, 7.6 Hz, 1H), 7.10 (d, J = 7.8 Hz, 1H), 7.04 (d, J = 7.7 Hz, 1H), 6.98 (dd, J = 1.3, 1.0 Hz, 1H), 4.73 (dd, J = 9.9, 5.8 Hz, 1H), 4.29 (ddd, J = 11.9, 5.5, 4.4 Hz, 1H), 4.14 (ddd, J = 11.9, 9.9, 5.1 Hz, 1H), 4.10 (s, 3H), 2.44 (dddd, J = 13.7, 6.0, 6.0, 2.6 Hz, 1H), 2.31 (d, J = 1.0 Hz, 3H), 2.29 (m, 1H), 2.13 (m, 1H), 1.91 (dddd, J = 13.6, 11.7, 8.7, 2.5 Hz, 1H); ^{13}C NMR (150 MHz, $CDCl_3$) δ 156.0, 154.0, 151.2, 149.6, 140.4, 138.7, 136.7, 132.5, 132.4, 132.1, 130.2, 128.5 (q, J_{C-F} = 29.7 Hz), 127.3, 126.2 (q, J_{C-F} = 5.5 Hz), 124.5 (q, J_{C-F} = 274.1 Hz), 121.7, 117.7, 115.8, 114.7, 55.8, 42.9, 37.0, 30.6, 21.6, 13.7; HRMS (ESI+) calcd for $C_{25}H_{24}F_3N_6O$ ($[M + H]^+$) 481.1958, found 481.1963.

Condensation and Cyclization of 10·HCl and (±)-23 (Table 3, Second-Generation Process). A reactor was charged with hydrazide **10**·HCl (132.0 kg, 362.4 mol) under a nitrogen atmosphere, and precooled MeOH (941.7 kg) at 10 °C was added. With stirring, NaOAc (208.1 kg, 2536.9 mol) and imidate HCl salt (±)-**23** (149.7 kg, 434.9 mol) were successively added, and the reactor wall was washed with MeOH (104.7 kg). After the mixture was stirred at 10−15 °C for 25 h, Et_3N (146.7 kg, 1449.7 mol) was added, and the mixture was warmed to 45 °C. After 60 h of stirring at 40−45 °C, the jacket temperature was set to 35 °C, and the mixture was diluted with *i*-PrOAc (1151.9 kg) followed by 5% aqueous NaCl (1320.0 kg) at 30−44 °C. After separation of the phases, MeOH (209.8 kg) was added to the organic layer, followed by washing with 5% aqueous NaCl (1319.8 kg) at 34−35 °C. To this mixture was added activated carbon (6.6 kg) in *i*-PrOAc (57.3 kg), and the mixture was stirred for 1 h at 32 °C. Celite (6.6 kg) in *i*-PrOAc (57.9 kg) was added, and the mixture was filtered through Celite (3.6 kg) followed by a rinse with *i*-PrOAc (95.5 kg). The filtered solution was concentrated under reduced pressure and then azeotroped with *i*-PrOH (207.2 kg × 3) at 16−45 °C (internal temperature). To the resulting solid was added *i*-PrOH (286.5 kg), and the mixture was heated to 61 °C to completely dissolve the solid. Then the mixture was cooled, and a seed crystal (30.1 g) was added at 55 °C. The mixture was cooled to 8 °C at a rate of 5 °C/h and held at 8 °C. The crystals were filtered and rinsed with an *i*-PrOH/*n*-heptane mixture (155.5 and 135.4 kg, respectively). The crystals were dried under reduced pressure at 60 °C to give crystals of the racemate (±)-**5** (136.6 kg, 78.5% yield from **10**·HCl) as a white powder.

Formation of the Diastereomeric Salt (*S*)-5·D-DPTA Using D-DPTA (Scheme 4). A reactor was charged D-DPTA (14.0 kg, 44.1 mol), MeOH (27.4 kg), and EtOAc (72.9 kg) under a nitrogen atmosphere, and the mixture was stirred and heated to 50 °C. To this mixture was added a solution of racemate (±)-**5** (38.5 kg, 80.1 mol, dissolved in MeOH (31.9 kg) and EtOAc (85.1 kg) at 55−60 °C in advance) over 1.5 h at 51−53 °C. (After addition of the first 20% of solution, seed crystals (5.1 g) were added, and then the remaining ∼80% of the

DOI: 10.1021/acs.oprd.8b00444
Org. Process Res. Dev. XXXX, XXX, XXX−XXX

solution was added). After completion of the addition, the reactor for racemate (±)-**5** was rinsed with MeOH (4.6 kg) and EtOAc (12.2 kg), and the rinses were added to the mixture. Then the mixture was stirred at 47−51 °C for 2 h, cooled to 8 °C at a rate of 10 °C/h, and held at 8 °C. The crystals were filtered and rinsed with a mixture of EtOAc and MeOH (125.0 and 12.2 kg) to give wet crystals (55.1 kg) and mother liquor 1 (327.6 kg). The wet crystals were charged to a reactor, and then MeOH (8.1 kg) and EtOAc (81.9 kg) were added. The mixture was then stirring and heated to 50 °C. After 3.5 h of stirring at 50−51 °C, the mixture was cooled to 8 °C at a rate of 5 °C/h and held at 8 °C. The crystals were filtered and rinsed with a mixture of EtOAc and MeOH (70.1 and 6.9 kg, respectively) to give wet crystals (45.8 kg) and mother liquor 2 (160.8 kg). The wet crystals were dried under reduced pressure at 60 °C for 18 h to give the D-DPTA salt (*S*)-**5**·D-DPTA (24.2 kg, 37.8% yield, 98.1% ee) as a white solid. Mother liquors 1 and 2 containing the undesired enantiomer (*R*)-**5**·D-DPTA were recycled according to the procedure described below. FTIR (cm^{-1}, KBr) 3676, 3426, 3191, 2975, 2484, 1725, 1476, 1311, 1160, 1062, 974, 779; ^{1}H NMR (600 MHz, $CDCl_3$) δ 8.34 (br s, 1H), 7.73 (d, J = 7.4 Hz, 1H), 7.65 (d, J = 15.7 Hz, 1H), 7.57 (d, J = 7.9 Hz, 1H), 7.48 (dd, J = 7.6, 7.4 Hz, 1H), 7.43 (d, J = 15.7 Hz, 1H), 7.40 (dd, J = 7.8, 7.6 Hz, 1H), 7.00 (d, J = 7.8 Hz, 1H), 6.99 (dd, J = 1.3, 1.1 Hz, 1H), 6.98 (d, J = 7.9 Hz, 1H), 5.91 (br s, 2H, OH), 5.55 (s, 2H), 4.70 (dd, J = 8.7, 5.8 Hz, 1H), 4.35 (ddd, J = 13.0, 5.8, 5.4 Hz, 1H), 4.35 (ddd, J = 13.0, 8.7, 4.9 Hz, 1H), 4.03 (s, 3H), 2.46 (dddd, J = 13.4, 6.6, 6.6, 2.0 Hz, 1H), 2.32 (d, J = 1.1 Hz, 3H), 2.27 (m, 1H), 2.16 (m, 1H), 1.95 (dddd, J = 13.5, 11.1, 8.5, 2.7 Hz, 1H), 1.20 (s, 9H); ^{13}C NMR (150 MHz, $CDCl_3$) δ 177.3, 169.7, 160.3, 155.7, 155.1, 152.3, 140.0, 135.8, 135.2, 133.4, 132.2, 131.0, 130.0, 128.4 (q, J_{C-F} = 29.9 Hz), 127.4, 126.4 (q, J_{C-F} = 5.6 Hz), 124.5 (q, J_{C-F} = 273.9 Hz), 123.0, 119.2, 117.1, 116.8, 71.4, 54.1, 50.7, 47.4, 38.7, 37.8, 31.1, 27.0, 21.3, 11.4; HRMS (ESI+) calcd for $C_{25}H_{24}F_3N_6O$ ($[M + H]^+$) 481.1958, found 481.1961, calcd for $C_{14}H_{21}O_8$ ($[M - H]^-$) 317.1242, found 317.1227; Chiral HPLC (CHIRALPAK IB 5 μm, 4.6 mm × 150 mm, 1.0 mL/min, mobile phase = 3:2 v/v *n*-hexane/EtOH, oven temperature = 25 °C, RRT of the undesired enantiomer (*R*)-**5** = 0.69.

E2212 (1). A reactor was charged with D-DPTA salt (*S*)-**5**·D-DPTA (22.0 kg, 27.5 mol), and EtOAc (198.4 kg) was added under a nitrogen atmosphere, after which stirring was started. To this mixture was added 5 N HCl (110.0 kg) at 16−17 °C with cooling. After the phases were separated, *i*-PrOAc (172.6 kg) and MeOH (17.4 kg) were added to the aqueous layer, which was cooled to 14 °C. To this mixture, 5 N NaOH (160.1 kg) was added at 14−26 °C to adjust the pH to 9.8 (the acceptable range is 7−10) and the aqueous layer was discarded. To the organic layer were added purified water (220.0 kg) and MeOH (8.7 kg), and the aqueous layer was discarded. To the organic layer were added purified water (110.0 kg) and MeOH (8.7 kg), and the aqueous layer was discarded. After MeOH (17.4 kg) was added to the organic layer, polish filtration of the resulting solution was performed, followed by rinsing with *i*-PrOAc (19.1 kg). The filtered solution was concentrated and azeotroped three times with *i*-PrOAc (38.4 kg, 57.5 kg, 57.5 kg) under reduced pressure at 23−53 °C (internal temperature) to give the free base (*S*)-**5**. To this were added *i*-PrOAc (87.7 kg) and *n*-PrOH (6.4 kg), and the mixture was heated to 73 °C to completely dissolve the solid. To this mixture was added a solution of D-tartaric acid (7.3 kg, 48.6 mol, dissolved in *n*-PrOH (47.9 kg) at 52 °C in advance) at 68−73 °C over 1 h. After completion of the addition, the container containing D-tartaric acid was rinsed with *n*-PrOH (6.4 kg), and the rinse was added to the mixture. Seed crystals (5.0 g) were added to the mixture, and then the mixture was stirred for 1 h at 70−71 °C, cooled to 8 °C at a rate of 10 °C/h, and held at 8 °C. The crystals were filtered and rinsed with a mixture of *n*-PrOH and *i*-PrOAc (10.3 and 22.3 kg) to give wet crystals (48.4 kg) and mother liquor 3 (148.0 kg). The wet crystals were dried under reduced pressure at 60 °C for 19.5 h to give E2212 (**1**) (18.0 kg, 92.5% yield) as a white solid. Mother liquor 3 were recycled according to the procedure described below. FTIR (cm^{-1}, KBr) 3461, 3173, 2956, 1734, 1584, 1536, 1476, 1309, 1130, 835, 765, 752; ^{1}H NMR (600 MHz, DMSO-d_6) δ 7.91 (s, 1H), 7.78 (d, J = 8.4 Hz, 1H), 7.77 (br d, J = 8.4 Hz, 1H), 7.61 (br dd, J = 7.8, 7.8 Hz, 1H), 7.49 (br dd, J = 7.8, 7.8 Hz, 1H), 7.46 (d, J = 15.6 Hz, 1H), 7.32 (d, J = 15.6 Hz, 1H), 7.27 (d, J = 7.8 Hz, 1H), 7.25 (br d, J = 7.8 Hz, 1H), 7.22 (s, 1H), 4.51 (dd, J = 9.0, 6.0 Hz, 1H), 4.29 (s, 3H), 4.28 (m, 2H), 3.98 (s, 3H), 2.29 (m, 1H), 2.14 (s, 3H), 2.16 (m, 2H), 1.96 (m, 1H); ^{13}C NMR (150 MHz, DMSO-d_6) δ 173.3, 159.3, 155.4, 155.0, 150.1, 141.1, 137.1, 136.9, 133.6, 132.9, 131.0, 130.5, 127.6, 127.1 (q, J_{C-F} = 30 Hz), 125.8 (q, J_{C-F} = 5.6 Hz), 124.7 (q, J_{C-F} = 270 Hz), 122.2, 120.7, 117.2, 116.5, 72.3, 53.7, 47.0, 37.6, 30.7, 21.3, 13.6; HRMS (ESI+) calcd for $C_{25}H_{23}F_3N_6O$ ($[M + H]^+$) 481.1958, found 481.1953.

Recovery of Racemate (±)-5 (Scheme 4). A reactor was charged with mother liquors 1 and 2 (assumed to be 49.9 mol in total) and mother liquor 3 (assumed to be 2.1 mol) described above under a nitrogen atmosphere, and the mixture was concentrated and azeotroped with *n*-PrOH three times (38.3 kg, 38.2 kg, 38.3 kg) under reduced pressure at 8−36 °C (internal temperature). To this mixture were added *n*-PrOH (38.3 kg) and 5 N NaOH (140.8 kg) followed by heating to 90 °C. After 49 h of stirring at 85−87 °C, the mixture was cooled to 45 °C, and the aqueous layer was discarded. To the organic layer were added *i*-PrOAc (41.5 kg) and water (95.3 kg). After the aqueous layer was discarded, the organic layer was washed with water (95.3 kg), and the aqueous layer was discarded. The organic layer was concentrated and azeotroped with *i*-PrOH (three times with 37.4 kg and then four times with 18.7 kg) under reduced pressure at 30−45 °C to give crude racemate (±)-**5**. To this mixture was added *i*-PrOH (37.9 kg), followed by heating to 70 °C to dissolve the solid. The mixture was cooled to 8 °C at a rate of 5 °C/h and held at 8 °C (seed crystals (16.6 g) were added when the internal temperature fell below 55 °C). The crystals were filtered and rinsed with a mixture of *i*-PrOH and *n*-heptane (28.0 and 24.4 kg, respectively) precooled at 0 °C to give wet crystals (20.7 kg). The wet crystals were dried under reduced pressure at 60 °C for 24 h to give racemate (±)-**5** (19.4 kg, 77.8% yield) as a pale-yellow solid. The reaction progress was monitored using the chiral HPLC conditions described above.

Photoisomerization of Olefin 1 in a Flow System. A solution of **1** (185.1 g, 262.3 mol) in MeCN (73.1 kg) and water (92.0 kg) was fed through PFE tubing (3.0 mm i.d., 0.5 mm thickness, 10 m length, wound around the photoreactor (Pyrex) equipped with a UV lamp) at a flow rate of 182 mL/min. The flow and irradiation were continued for 17 h with occasional monitoring of the flow rate and *E*/*Z* ratio. The temperature of the cooling medium was kept at −5 to −1 °C during flow (after 9 h, feeding of the solution of **1** was stopped, and 50% aqueous MeCN was fed at 182 mL/min for 3 min to wash the flow system and then turned off; the flow was resumed the following day). The isomerized product eluted from outlet of the PFE tubing was concentrated under reduced temperature below 42 °C

DOI: 10.1021/acs.oprd.8b00444
Org. Process Res. Dev. XXXX, XXX, XXX−XXX

(internal temperature), and the residue was azeotroped with *n*-PrOH twice (500 mL, 300 mL) to give an *E*/*Z* mixture of E2212 (196.0 g (containing residual *n*-PrOH), *E*:*Z* = 61.8:37.4 by UV (271 nm), 1.3:1.0 by ^{1}H NMR) as an orange oil. HPLC conditions to monitor the isomerization conversion and *E*/*Z* ratio: XBridge-Shield-RP18 (5 μm, 4.6 mm × 250 mm), 1.0 mL/min, oven temperature = 40 °C, mobile phase A = 900:100:1 v/v/w H_2O/MeCN/$AcONH_4$, mobile phase B = 100:900:1 v/v/w H_2O/MeCN/$AcONH_4$, gradient (time (min)/B conc (%)) = 0/5 → 5/45 → 35/45 → 50/100 → 55/100 → 55.01/5 → 65/5 → 65.01/stop, RRT of *Z* form = 0.73.

From this mixture, a small portion was purified by silica gel column chromatography to give the *Z* isomer in free form. FTIR (cm^{-1}, KBr) 3416, 2952, 1586, 1500, 1487, 1313, 1161, 1114, 1036, 966, 858, 769; ^{1}H NMR (600 MHz, $CDCl_3$) δ 7.90 (d, *J* = 7.9 Hz, 1H), 7.72 (d, *J* = 1.2 Hz, 1H), 7.70 (d, *J* = 7.9 Hz, 1H), 7.45 (dd, *J* = 7.6, 7.4 Hz, 1H), 7.37 (dd, *J* = 7.7, 7.6 Hz, 1H), 7.30 (d, *J* = 7.9 Hz, 1H), 7.02 (d, *J* = 7.9 Hz, 1H), 6.93 (dd, *J* = 1.2, 1.0 Hz, 1H), 6.73 (d, *J* = 13.3 Hz, 1H), 6.64 (d, *J* = 13.3 Hz, 1H), 4.63 (dd, *J* = 9.3, 5.9 Hz, 1H), 4.34 (br ddd, *J* = 13.0, 5.6, 4.1 Hz, 1H), 4.28 (ddd, *J* = 13.0, 9.9, 4.9 Hz, 1H), 3.92 (s, 3H), 2.45 (dddd, *J* = 13.2, 6.5, 6.5, 2.6 Hz, 1H), 2.29 (d, *J* = 1.0 Hz, 3H), 2.28 (m, 1H), 2.15 (m, 1H), 1.94 (dddd, *J* = 12.9, 11.4, 8.3, 2.6 Hz, 1H); ^{13}C NMR (150 MHz, $CDCl_3$) δ 159.4, 155.2, 154.4, 150.8, 140.2, 138.3, 136.6, 133.2, 131.9 131.6, 129.9, 128.5 (q, J_{C-F} = 29.8 Hz), 127.2, 126.2 (q, J_{C-F} = 5.6 Hz), 124.4 (q, J_{C-F} = 274.0 Hz), 121.8, 120.1, 118.4, 116.0, 53.6, 47.3, 37.9, 31.0, 21.7, 13.6; HRMS (ESI+) calcd for $C_{25}H_{24}F_3N_6O$ ($[M + H]^+$) 481.1958, found 481.1960.

■ ASSOCIATED CONTENT

Supporting Information

The Supporting Information is available free of charge on the ACS Publications website at DOI: 10.1021/acs.oprd.8b00444.

^{1}H and ^{13}C NMR, FT-IR, and HRMS characterization data and representative HPLC data of key compounds ((±)-**5**, (*S*)-**5**·D-DPTA, **1**, and the (*Z*)-olefin) and impurities (regioisomer (±)-**28**, oxadiazole (±)-**29**) (PDF)

■ AUTHOR INFORMATION

Corresponding Authors

*E-mail: m-isomura@hhc.eisai.co.jp.
*E-mail: k-tagami@hhc.eisai.co.jp.

ORCID

Minetaka Isomura: 0000-0002-7344-5129

Notes

The authors declare no competing financial interest.

■ ACKNOWLEDGMENTS

We are grateful to Hiroki Matsunaga for analytical support.

■ REFERENCES

(1) For a recent report on Alzheimer's disease, see: Alzheimer's Association. 2018 Alzheimer's disease facts and figures. *Alzheimer's Dementia* **2018**, *14*, 367.

(2) For a recent review of the amyloid hypothesis, see: Selkoe, D. J.; Hardy, J. The amyloid hypothesis of Alzheimer's disease at 25 years. *EMBO Mol. Med.* **2016**, *8*, 595.

(3) Yu, Y.; Logovinsky, V.; Schuck, E.; Kaplow, J.; Chang, M.-K.; Miyagawa, T.; Wong, N.; Ferry, J. Safety, tolerability, pharmacokinetics, and pharmacodynamics of the novel γ-secretase modulator, E2212, in healthy human subjects. *J. Clin. Pharmacol.* **2014**, *54*, 528.

(4) Kimura, T.; Kitazawa, N.; Kaneko, T.; Sato, N.; Kawano, K.; Ito, K.; Takaishi, M.; Sasaki, T.; Yoshida, Y.; Uemura, T.; Doko, T.; Shinmyo, D.; Hasegawa, D.; Miyagawa, T.; Hagiwara, H. Polycyclic Compound. WO2009028588, 2009.

(5) Kamada, A.; Sasaki, T.; Uemura, T. Method for Producing Polycyclic Compound and Intermediate for Same. WO2010098332, 2010.

(6) Uemura, T.; Sasaki, T.; Hoshino, Y.; Isomura, M. Process for Producing Tetrahydrotriazolopyridine Derivative. WO2010098496, 2010.

(7) Burnett, D. A.; Bursavich, M. G.; McRiner, A. J. Fused Morpholinopyrimidines and Methods of Use Thereof. WO2015109109, 2015.

(8) It was difficult to obtain optical purity data for cyclic amidine (*S*)-**8**. Therefore, racemization from (*S*)-**18** to (*S*)-**8** cannot be excluded in route B.

(9) Nakamura, T.; Matsuda, M.; Hu, Y.; Hasegawa, D.; Hoshino, Y.; Inanaga, K.; Isomura, M.; Sato, N.; Yoshizawa, K.; Moniz, G. A.; Wilkie, G. D.; Fang, F. G.; Nishikawa, Y. Process for Preparing Certain Cinnamide Compounds. WO2010025197, 2010.

(10) During the process studies, the structure of the imidate was changed from Me-imidate (±)-**19** to Et-imidate (±)-**23** because of its improved stability. The salt form of hydrazide **10** was also changed from free to dihydrochloride hydrate.

(11) Hook, B. D. A.; Dohle, W.; Hirst, P. R.; Pickworth, M.; Berry, M. B.; Booker-Milburn, K. I. A Practical Flow Reactor for Continuous Organic Photochemistry. *J. Org. Chem.* **2005**, *70*, 7558.

DOI: 10.1021/acs.oprd.8b00444
Org. Process Res. Dev. XXXX, XXX, XXX−XXX